This is the peer reviewed version of the following article :NLRP3 inflammasome as prognostic factor and therapeutic target in primary progressive multiple sclerosis patients. Sunny Malhotra,1 Carme Costa,1 Herena Eixarch,1 Christian W. Keller,2,3 Lukas Amman,4,5 Helios Mart´ınez-Banaclocha,6 Luciana Midaglia,1 Eduard Sarro´,7 Isabel Mach´ın-D´ıaz,8 Luisa M. Villar,9 Juan Carlos Trivin~o,10 Begon~a Oliver-Martos,11 Laura Navarro Parlade´,1 Laura Calvo-Barreiro,1 Fuencisla Matesanz,12 Koen Vandenbroeck,13,14 Elena Urcelay,15 Mar´ıa-Luisa Mart´ınez-Gine´s,16 Amalia Tejeda-Velarde,9 Nicola´s Fissolo,1 Joaqu´ın Castillo´,1 Alex Sanchez,17,18 Avril A.B. Robertson,19 Diego Clemente,8 Marco Prinz,4,20,21 Pablo Pelegrin,6 Jan D. Lu¨ nemann,2,3 Carmen Espejo,1 Xavier Montalban1,22 and Manuel Comabella1. Brain . 2020 May 1;143(5):1414-1430 which has been published in final form at 10.1093/brain/awaa084.

NLRP3 inflammasome as prognostic factor and therapeutic target in primary progressive multiple sclerosis patients

Sunny Malhotra,[1] Carme Costa,[1] Herena Eixarch,[1] Christian W. Keller,[2,3] Lukas Amman,[4,5] Helios Mart´ınez-Banaclocha,[6] Luciana Midaglia,[1] Eduard Sarró,[7] Isabel Mach´ın-D´ıaz,[8] Luisa M. Villar,[9] Juan Carlos Trivi˜no,[10] Begoña Oliver-Martos,[11] Laura Navarro Parladé,[1] Laura Calvo-Barreiro,[1] Fuencisla Matesanz,[12] Koen Vandenbroeck,[13,14] Elena Urcelay,[15] Mar´ıa-Luisa Mart´ınez-Ginés,[16] Amalia Tejeda-Velarde,[9] Nicolás Fissolo,[1] Joaqu´ın Castilló,[1] Alex Sanchez,[17,18] Avril A.B. Robertson,[19] Diego Clemente,[8] Marco Prinz,[4,20,21] Pablo Pelegrin,[6] Jan D. L ü nemann,[2,3] Carmen Espejo,[1] Xavier Montalban[1,22] and Manuel Comabella[1]

Primary progressive multiple sclerosis is a poorly understood disease entity with no specific prognostic biomarkers and scarce therapeutic options. We aimed to identify disease activity biomarkers in multiple sclerosis by performing an RNA sequencing approach in peripheral blood mononuclear cells from a discovery cohort of 44 untreated patients with multiple sclerosis belonging to different clinical forms and activity phases of the disease, and 12 healthy control subjects. A validation cohort of 58 patients with multiple sclerosis and 26 healthy control subjects was included in the study to replicate the RNA sequencing findings. The RNA sequencing revealed an interleukin 1 beta (IL1B) signature in patients with primary progressive multiple sclerosis. Subsequent immunophenotyping pointed to blood monocytes as responsible for the IL1B signature observed in this group of patients. Functional experiments at baseline measuring apoptosis-associated speck-like protein containing a CARD (ASC) speck formation showed that the NOD-leucine rich repeat and pyrin containing protein 3 (NLRP3) inflammasome was overactive in monocytes from patients with primary progressive multiple sclerosis, and canonical NLRP3 inflammasome activation with a combination of ATP plus lipopolysaccharide was associated with increased IL1B production in this group of patients. Primary progressive multiple sclerosis patients with high *IL1B* gene expression levels in peripheral blood mononuclear cells progressed significantly faster compared to patients with low *IL1B* levels based on the time to reach an EDSS of 6.0 and the Multiple Sclerosis Severity Score. In agreement with peripheral blood findings, both NLRP3 and IL1B expression in brain tissue from patients with primary progressive multiple sclerosis was mainly restricted to cells of myeloid lineage. Treatment of mice with a specific NLRP3 inflammasome inhibitor attenuated established experimental autoimmune encephalomyelitis disease severity and improved CNS histopathology. NLRP3 inflammasome-specific inhibition was also effective in reducing axonal damage in a model of lipopolysaccharide-neuroinflammation using organotypic cerebellar cultures. Altogether, these results point to a role of IL1B and the NLRP3 inflammasome as prognostic biomarker and potential therapeutic target, respectively, in patients with primary progressive multiple sclerosis.

1 Servei de Neurologia-Neuroimmunologia, Centre d'Esclerosi Mu´ltiple de Catalunya (Cemcat), Institut de Recerca Vall d'Hebron (VHIR), Hospital Universitari Vall d'Hebron, Universitat Auto`noma de Barcelona, Barcelona, Spain
2 Department of Neurology with Institute of Translational Neurology, University Hospital Mu¨nster, Mu¨nster, Germany

3 Institute of Experimental Immunology, Laboratory of Neuroinflammation, University of Zurich, Zurich, Switzerland

4 Institute of Neuropathology, Medical Faculty, University of Freiburg, Freiburg, Germany
5 Faculty of Biology, University of Freiburg, Freiburg, Germany
6 Biomedical Research Institute of Murcia (IMIB-Arrixaca), University Clinical Hospital Virgen de la Arrixaca, Murcia, Spain
7 Renal Physiopathology Group, Institut de Recerca Vall d'Hebron (VHIR) - CIBBIM Nanomedicine, Barcelona, Spain
8 Grupo de Neuroinmuno-Reparacio´n, Hospital Nacional de Paraple´jicos-SESCAM, Toledo, Spain
9 Departments of Immunology and Neurology, Multiple Sclerosis Unit, Hospital Ramon y Cajal, (IRYCIS), Madrid, Spain
10 Genomic Systems, Valencia, Spain
11 Neuroimmunology and Neuroinflammation Group, Instituto de Investigacio´n Biome´dica de Ma´laga-IBIMA, UGC Neurociencias, Hospital Regional Universitario de Ma´laga, Ma´laga, Spain
12 Department of Cell Biology and Immunology, Instituto de Parasitologı´a y Biomedicina "Lo´pez Neyra", Consejo Superior de Investigaciones Cientı´ficas (IPBLN-CSIC), Granada, Spain
13 Universidad del Paı´s Vasco (UPV/EHU), Leioa, Spain
14 IKERBASQUE, Basque Foundation for Science, Bilbao, Spain
15 Hospital Cl´ınico San Carlos, Instituto de Investigacio´n Sanitaria San Carlos (IdISSC), Madrid, Spain
16 Department of Neurology, Hospital General Universitario Gregorio Marañón, Madrid, Spain
17 Department of Genetics, Microbiology and Statistics, Universitat de Barcelona, Barcelona, Spain
18 Statistics and Bioinformatics Unit, Vall d'Hebron Institut de Recerca, Barcelona, Spain
19 School of Chemistry and Molecular Biosciences, University of Queensland, Brisbane, Australia
20 Signalling Research Centres BIOSS and CIBSS, University of Freiburg, Freiburg, Germany
21 Center for NeuroModulation (NeuroModul), Faculty of Medicine, University of Freiburg, Freiburg, Germany
22 Center for Multiple Sclerosis, St, Michael's Hospital, University of Toronto, Toronto, ON, Canada

Correspondence to: Manuel Comabella
Unitat de Neuroimmunologia Cl´nica, Cemcat. Hospital Universitari Vall d'Hebron. Pg. Vall d'Hebron 119-129 08035 Barcelona, Spain
E-mail: manuel.comabella@vhir.org

Correspondence may also be addressed to: Sunny Malhotra
E-mail: sunnymalhotra4u24@gmail.com

Keywords: multiple sclerosis; biomarkers; therapeutic target; NLRP3 inflammasome; prognostic factor

Abbreviations: EAE = experimental autoimmune encephalomyelitis; EDSS = Expanded Disability Status Scale; IFN = interferon; MSSS = Multiple Sclerosis Severity Score; PBMC = peripheral blood mononuclear cell; ROMS = relapse-onset multiple sclerosis; RNA-seq = RNA sequencing; RRMS = relapsing-remitting multiple sclerosis; SPMS = secondary progressive multiple sclerosis; PPMS = primary progressive multiple sclerosis

Introduction

Biomarkers are objectively measured indicators of normal processes or pathological conditions (Biomarkers Definitions Working Group *et al.* 2001). They are particularly needed in multiple sclerosis, a disease of complex aetiopathogenesis characterized by a high degree of multi-nature heterogeneity at the clinical, radiological, pathological, and treatment response levels (Lublin and Reingold, 1996; Lucchinetti *et al.*, 2000; Bielekova *et al.*, 2005; Bermel *et al.*, 2013). In this context, biomarkers in multiple sclerosis may help to distinguish between different clinical courses with distinct prognoses and, more importantly, they might become therapeutic targets that set the rationale for the design of new or effective therapies for the disease (Comabella and Montalban, 2014). Keeping these needs and limitations in mind, in the present study we embarked on a study aimed at identifying disease activity biomarkers in multiple sclerosis using a genome-wide technique, RNA sequencing (RNA-seq), and found interleukin 1 beta (IL1B) and the NOD-leucine rich repeat and pyrin containing protein 3 (NLRP3) inflammasome as prognostic factor and potential therapeutic target, respectively in multiple sclerosis patients with primary progressive disease course (PPMS).

Materials and methods

Discovery cohort

The discovery cohort comprised 44 patients with untreated multiple sclerosis and 12 healthy controls. The multiple sclerosis group included: (i) 10 patients with early relapsing-remitting multiple sclerosis (RRMS) and active disease (in the first 5 years after disease onset and fulfilling criteria for treatment with immunomodulators); (ii) 11 RRMS patients with benign disease course [defined by the presence of Expanded Disability Status Scale (EDSS) scores 4 3.0 after 515 years from disease onset]; (iii) 12 patients with secondary progressive multiple sclerosis (SPMS; patients with relapsing-remitting disease onset who experienced disability progression not related to relapses, quantified as a confirmed increase at 6 months in the EDSS of 1 point if EDSS 5 5.5 and 0.5 points if EDSS 5 5.5); and (iv) 11 patients with PPMS. None of these patients had ever received treatment with immunosuppressive or immunomodulatory

therapies. A summary of demographic and main clinical characteristics is shown in Supplementary Table 1.

RNA sequencing

RNA-seq was performed in peripheral blood mononuclear cells (PBMCs) from individuals included in the discovery cohort. Library preparation and computational analysis of RNA-seq are summarized in the Supplementary material.

Multiple sclerosis validation cohort

An independent cohort of 58 untreated multiple sclerosis patients who never previously received immunosuppressive or immunomodulatory therapies and 26 healthy control subjects was used to validate the RNA-seq findings by an alternative technique, real-time PCR. The multiple sclerosis group included 22 patients with RRMS, 16 patients with SPMS, and 20 patients with PPMS. Considering that benign patients were having a RRMS disease course and findings in RNA-seq were similar to the RRMS group, patients with benign disease were not included in the validation cohort. Similarly, considering that RRMS and SPMS patients have both a relapse onset and that RNA-seq findings were similar between both groups of patients, these two patient categories were merged as relapse-onset multiple sclerosis (ROMS). Supplementary Table 2 summarizes demographic and main clinical characteristics of this validation cohort. In a subgroup of PPMS patients belonging to this validation cohort (n = 12), brain MRI scans were performed in proximity to PBMC collection (46 months) and information on T_1 and T_2 lesion loads was available. These patients participated in a phase II randomized, double-blind, placebo-controlled trial of interferon (IFN)-b (Montalban *et al.*, 2009) and were included in the placebo arm.

PPMS validation cohort

An independent cohort of 21 PPMS patients was included to validate the prognostic implications of high *IL1B* mRNA expression levels in PBMCs. These patients had never received immunosuppressive or immunomodulatory therapies before blood collection and remained untreated until the time of the last follow-up included in the study. Demographic and main clinical characteristics are summarized in Supplementary Table 3.

For both discovery and validation cohorts, all patients with multiple sclerosis were followed prospectively every 3–6 months and presence of relapses and EDSS scores were collected at each visit.

Real-time PCR to measure *IL1B*, *NLRP3*, *IL6*, and *TNF* expression levels

In individuals included in the validation cohort, total RNA was extracted from PBMCs previously frozen in liquid nitrogen by means of an RNeasy® kit (Qiagen) and cDNA synthesized with the High Capacity cDNA Archive kit (Applied Biosystems). Messenger RNA expression levels for *IL1B*, *NLRP3*, *IL6* and *TNF* were determined by real-time PCR using TaqMan® probes specific for each gene (Applied Biosystems). The housekeeping gene glyceraldehyde-3-phosphate dehydrogenase (*GAPDH*) was used as an endogenous control (Applied Biosystems). Assays were run on the ABI PRISM® 7900HT system (Applied Biosystems) and data were analysed using the 2–DDCT method (Livak and Schmittgen, 2001). Results were expressed as fold-change in gene expression in patients with PPMS, SPMS, and RRMS relative to healthy control subjects (calibrators), and in patients during relapses relative to patients in clinical remission (calibrators).

Assessment of time to reach EDSS 6.0

Time to reach EDSS 6.0 (confirmed at 6 months) in patients with PPMS and ROMS with high and low mRNA expression levels of *NLRP3* and *IL1B* according to a cut-off value based on the median were evaluated by Kaplan–Meier survival analysis with the log-rank test.

Peripheral blood cell immunophenotyping and flow cytometry analysis

Expression of intracellular cytokines (IL1B, TNF, IL6) and NLRP3, CD40, CD80, CD86, and PD-L1 within PBMC subsets [monocytes, BDCA-1- and BDCA-3-positive dendritic cells, plasmacytoid dendritic cells, B cells, T cells, CD56dimCD16 + natural killer (NK) cells, CD56hiCD16neg NK cells, CD14 + CD16neg, CD14 + CD16 + , and CD14negCD16 + monocytes] was analysed by flow cytometry in a subgroup of 31 multiple sclerosis patients and 11 healthy control subjects belonging to the discovery and validation cohorts. The multiple sclerosis group comprised 10 patients with PPMS and 21 patients with ROMS. A summary of demographic and clinical characteristics is provided in Supplementary Table 4. Immunophenotyping and flow cytometry analysis methods are summarized in the Supplementary material. Supplementary Fig. 1 depicts gating strategy and Supplementary Fig. 2 shows representative density plots and histograms for IL1B, IL6, TNF, and NLRP3 expression in monocytes.

Quantification of IL1B levels in serum samples by ELISA

Levels of IL1B were measured in serum samples of 81 multiple sclerosis patients and 16 healthy control subjects belonging to the discovery and validation cohorts. The multiple sclerosis group included 30 patients with PPMS and 51 patients with ROMS (SPMS and RRMS). Supplementary Table 4 summarizes demographic and clinical characteristics of patients. Serum samples were obtained at the same time as the PBMCs used in the expression studies. Briefly, peripheral blood was collected by standard venipuncture and allowed to clot spontaneously for 30 min. Serum was isolated by centrifugation and stored frozen at –80ºC until used. IL1B levels were measured in serum samples by means of a commercially available ELISA (Human IL1B ELISA; R&D Systems). Samples were measured in duplicate in undiluted serum. The intra-assay and inter-assay coefficients of variation were 5.8% and 8.4%, respectively.

CSF monocytes immunophenotyping and flow cytometry analysis

Expression of intracellular IL1B was measured by flow cytometry in CSF samples from nine untreated multiple sclerosis patients, three with PPMS and six with ROMS. A summary of demographic and clinical variables of patients is provided in Supplementary Table 4.

Quantification of baseline active caspase-1 and ASC speck formation in monocytes

Caspase-1 activity and ASC speck formation was determined in PBMCs from PPMS patients (n = 5), ROMS patients (n = 5), and healthy control subjects (n = 4). Intracellular apoptosis-associated speck-like protein containing a CARD (ASC) speck formation was evaluated by the time of flight inflammasome evaluation (TOFIE) in CD14 + monocytes using a polyclonal unconjugated rabbit anti-ASC (N-15)-R antibody (Santa Cruz Biotechnology) and a secondary monoclonal donkey anti-rabbit antibody Alexa Fluor® 488 (Thermo Fisher Scientific), both at 1:1000 dilution. Active caspase-1 was measured in monocytes using the specific fluorescent probe FLICA-660 Caspase-1 Assay Kit (Immunochemistry Technologies) following the manufacturer's instructions. For the determination of ASC specks and FLICA, monocytes were selected using anti-CD14 PE (clone 61D3, Tonbo Biosciences) or anti-CD14 APC-H7 (clone MuP9, BD Biosciences), respectively. Samples were analysed by flow cytometry using a FACS Canto (BD Biosciences) and the FCS express software (De Novo Software). Supplementary Fig. 3 summarizes the gating strategy.

Canonical NLRP3 inflammasome activation and quantification of IL1B levels in supernatant by ELISA

Canonical activation of the NLRP3 inflammasome is illustrated in Supplementary Fig. 4. PBMCs from PPMS patients (n = 9), ROMS patients (n = 7), multiple sclerosis patients whose blood was collected at the time of clinical relapses (relapsing patients; n = 3), and healthy control subjects (n = 7) were plated at a density of 10^6 cells/well and left untreated or primed with lipopolysaccharide (LPS, 1 lg/ll; Sigma) for 3 h and subsequently activated with ATP (5 mM; InvivoGen) for one additional hour. For some culture conditions, PBMCs were incubated in the presence of IFNb (100 IU/ml) or IL-10 (100 ng/ml; ThermoFisher Scientific) for 4 h and then the inflammasome activated as previously described with LPS and ATP. After stimulation, supernatants were collected following centrifugation of the cultured PBMCs and stored frozen at –80ºC until used. IL1B levels were measured in supernatants by ELISA as previously described. The intra-assay and inter-assay coefficients of variation were 5.1% and 9.2%, respectively.

Western blot analysis to determine NF-jB and IL1B intracellular expression

NF-jB expression was measured in unstimulated conditions in PBMCs from PPMS patients (n = 4), ROMS patients (n = 4) and healthy control subjects (n = 4). Intracellular IL1B expression was determined in PBMCs from PPMS patients (n = 4), ROMS patients (n = 4), relapsing patients (n = 3), and healthy control subjects (n = 3) after NLRP3 inflammasome activation with a combination of LPS + ATP, as described above. For western blot analysis, PBMCs were lysed in RIPA buffer supplemented with protease inhibitor cocktail (Sigma-Aldrich). Protein concentration was determined by the BCA assay (Thermo Fisher Scientific) and equal amounts of protein were run on SDS-PAGE gels and transferred onto PVDF membranes. Membranes were blocked with 5% non-fat dry milk for 1 h at room temperature and incubated overnight at 4ºC with specific primary antibodies against NF-jB p65 (sc-372, Santa Cruz Biotechnology), IL1B (ab2105, Abcam) and actin (A5060, Sigma-Aldrich). Membranes were then incubated with the appropriate secondary horseradish-peroxidase-labelled antibody and developed with the enhanced chemiluminescence method (Millipore). Finally, blots were imaged on an Odyssey Fc imager (LI-COR, Lincoln, NE) and bands were quantified with the Image Studio Lite software (LI-COR). A representative western blot is shown in Supplementary Fig. 5.

Quantification of NF-jB p65 transcription factor activity

NF-jB activity was measured in unstimulated conditions in nuclear protein extracts of PBMCs from the same PPMS patients (n = 4), ROMS patients (n = 4) and healthy control subjects (n = 4) that were used to determine NF-jB expression by western blot. Nuclear proteins were extracted from PBMCs by means of a commercially available Nuclear Extraction Kit (Ray Biotech; Catalogue: NE-50) and stored frozen at –80ºC until used. NF-jB p65 transcription factor activity assay was performed by means of a commercially available assay (Human NF-kB p65 Transcription Factor Activity Assay Kit; Ray Biotech; Catalogue: TFEH-p65), according to the manufacturer's instructions.

Genotyping of the *NLRP3* polymorphism

Genomic DNA from peripheral blood samples was obtained using standard methods from 2031 individuals including patients with PPMS (n = 309), patients with ROMS (n = 695), and healthy control subjects (n = 1027). Genotyping of rs35829419 was performed by means of the 5^0 nuclease assay technology for allelic discrimination using fluorogenic TaqMan® probes on a 7900 Applied Biosystems machine. Rs35829419 was commercially available from Applied Biosystems through the Assay-on-Demand service.

Human brain tissue samples

Paraffin-embedded brain samples from PPMS patients and non-neurological controls were provided by the UK Multiple Sclerosis

Tissue Bank (Imperial College London). Tissue sections were stained with haematoxylin and eosin and Klu¨ ver-Barrera for inflammation and demyelination assessment. Two brain tissue samples were selected for the study. First, samples from PPMS patients. In this group, all lesions showed an inactive core with a variable inflammatory activity at the border. For this reason, all lesions, based on their activity at the border, were subsequently classified into two groups as mixed active/inactive demyelinating lesions (n= 7) [when macrophages/microglia were observed only at the lesion border and Luxol fast blue (LFB) + degradation products were observed within macrophages/microglia] and mixed active/inactive post-demyelinating lesions (n= 5) (when macrophages/microglia were observed only at the lesion border and LFB + degradation products were not observed within macrophages/microglia), according to the criteria published by Kuhlmann *et al.* (2017). The second group of samples comprised brain tissue from non-neurological controls (n= 5).

NLRP3 and IL1B immunohistochemistry and immunostaining assessment

Immunostainings were developed with the automated Benchmark XT platform from Ventana Medical System. Briefly, 4-mm thick, paraffin-embedded serial sections were deparaffinized with EZ Prep™ (Ventana Medical Systems). Antigen retrieval was performed with Cell Conditioning 1 pH 8 (Ventana Medical Systems), for 30 min. Endogenous peroxidase activity was blocked with hydrogen peroxide 3%. Samples were incubated with the following primary antibodies: rabbit anti-NLRP3 (Abcam ab214185) and rabbit anti-IL1B (Abcam ab82558) for 36 min and visualized with ultraView Universal DAB (Ventana Medical Systems). All samples were counterstained with haematoxylin.

For each multiple sclerosis sample, five pictures were taken. Total NLRP3- and IL1B-positive cells were counted. Percentages of positive cells were calculated with respect to the total number of cells. Myelin basic protein (MBP) immunostainings were performed with the automated Autostainer Plus from Dako. In brief, antigen retrieval was performed at pH 6 prior to blocking endogenous peroxidases. Rabbit anti-MBP (Dako A0623) antibody was incubated overnight and visualized with EnVision detection system DAB (Dako SM809). For double immunostainings, antigen retrieval was performed at pH 6 prior to blocking endogenous peroxidase activity. Afterwards, sections were blocked for 10 min with 10% normal donkey serum to prevent unspecific binding of the antibodies. Primary antibodies (anti-NLRP3 or anti-IL1B) were incubated at 4ºC overnight and visualized with EnVision detection system DAB (Dako SM809). Before addition of the primary rabbit anti-IBA1 (Abcam ab178846) or rabbit anti-TMEM119 (Abcam ab185333) antibodies, sections were again blocked with hydrogen peroxide 3% and 10% normal goat serum as described before. The antibodies were incubated at 4ºC overnight and visualized with the Monosan Permanent-AP Red Kit (Monosan MON-APP185).

Mouse EAE induction, clinical follow-up and treatment

Eight-week-old female C57BL6/J mice were immunized with myelin oligodendrocyte glycoprotein (MOG)35-55 as described in the Supplementary material. At Days 13–14 post-immunization, mice were injected intraperitoneally daily with a NLRP3 inflammasome inhibitor (MCC950) (Coll *et al.*, 2015) (50 mg/kg or 100 mg/kg), 100 mg/kg of an IL1R antagonist (anakinra, Kineret®) or vehicle (200 ll of PBS). Treatment administration and clinical follow-up were performed in a blinded manner. Experimental autoimmune encephalomyelitis (EAE) clinical severity was analysed by means of area under the curve.

Time course of *Nlrp3* and *Il1b* gene expression in spinal cord from EAE mice

C57BL6/J mice were immunized as described above, sacrificed at 8, 16, 22, 29, 36, and 50 days post-immunization and spinal cord tissue obtained. *Nlrp3* and *Il1b* gene expression was determined by real-time PCR (Supplementary material).

Splenocyte proliferative assay and IL17 production

Splenocytes were stimulated with MOG35-55 or phytohaemagglutinin (PHA) and incorporated ^{3}H-thymidine was measured as described in the Supplementary material. IL17 production was determined in the supernatants of MOG35-55-stimulated splenocytes with Mouse IL17 Platinum ELISA (Affymetrix eBioscience; BMS6001), according to the manufacturer's instructions.

Histopathology and immunohistochemistry in EAE and treated mice

The animals were euthanized by CO_2 asphyxiation and the brains and spinal cords were removed and fixed with 4% paraformaldehyde (Sigma-Aldrich) for 24 h. The entire brains were cut in four coronal sections and the whole spinal cords were cut in two coronal and two transversal sections, which were embedded in paraffin wax, obtaining one paraffin block for every mouse. Brains and spinal cords were cut into 4-lm thick serial sections. Histopathological assessment was developed in slides containing two coronal and two longitudinal sections of the spinal cord for every mouse. Supplementary Fig. 6 shows examples of zoomed-out images representative of the spinal cord sections that were used for histological evaluation. Cell infiltration (haematoxylin and eosin staining) was evaluated according to the following criteria: 0, no lesion; 1, cellular infiltration only in the meninges; 2, very discrete and superficial infiltrates in the parenchyma; 3, moderate infiltrates (525%) in the white matter; 4, severe infiltrates (25–50%) in the white matter; and 5, more severe infiltrates (450%) in the white matter. Demyelination (Klu¨ ver-Barrera staining) was scored as follows: 0, no demyelination; 1, little demyelination only around infiltrates and involving 525% of the white matter; 2, demyelination involving 550% of the white matter; and 3, diffuse and widespread demyelination involving 450% of the white matter. Quantification studies were done by selecting five representative areas (0.25 mm^2) of the white matter after examining all the spinal cord areas (two coronal and two longitudinal sections) included in every slice. Double immunostainings were

performed to investigate NLRP3 and IL1B expression in astrocytes (GFAP +), macrophages/microglial cells [*Lycopersicon esculentum* agglutinin (LEA +)], and neurons (NeuN +) (Supplementary material).

Organotypic cerebellar slice cultures

Cerebellar slice cultures were prepared from 7-day-old C57BL/l6 mice from both sexes. Briefly, 300 mm parasagittal slices of cerebellum were obtained using a McIlwain tissue chopper (Ted Pella, Inc.). The slices were prepared from litters of five to seven pups and randomly distributed between conditions. Between six and eight slices were grown on each 0.4-lm cell culture insert (Millicell PICMORG50) in a P6 culture plaque, adding 1 ml/well of medium containing 50% Basal medium containing Earle's salt (BME, Gibco), 25% Hank's buffered salt solution (HBSS; Gibco), 25% inactivated horse serum (Gibco), 5 mg/ml glucose, 0.25 mM L-glutamine (Gibco) and 25 mg/ml penicillin/streptomycin (Gibco), and incubated at 37ºC, 5% CO_2. In all experiments, cerebellar slices were maintained for 7 days in culture to reduce microglia activation and allow myelination before starting the studies. Culture medium was refreshed every 2 days. Cultures were then treated with 15 lg/ml of LPS (Sigma), a concentration known to induce axonal damage (di Penta *et al.*, 2013), alone or together with different doses (1, 5 and 10 lM) of the specific NLRP3 inflammasome inhibitor (MCC950) for 24 h. Cerebellar slices maintained in culture medium alone were included to establish basal axonal damage level. Immunofluorescence microscopy to evaluate axonal damage is summarized in the Supplementary material.

Ethics statement for human and animal studies

All human studies were approved by the corresponding local ethics committees and participants gave written informed consent. All animal experiments were carried out in strict accordance with the EU and governmental regulations. The Ethics Committee on Animal Experimentation of the Hospital Universitari Vall d'Hebron and the Hospital Nacional de Paraple´jicos approved all procedures described in this study. All the data presented here are in accordance with the guidelines suggested for EAE publication (Baker and Amor, 2012).

Data availability

The data that support the findings of the study are available from the corresponding author upon reasonable request.

Results

RNA-seq reveals a pro-inflammatory signature in patients with PPMS characterized by upregulation of *IL1B* and *NLRP3*

RNA-seq was first performed in PBMCs from a discovery cohort of healthy control subjects and multiple sclerosis patients belonging to different clinical forms and activity phases of the disease. A pro-inflammatory signature composed of cytokine and chemokine genes was consistently upregulated in all the comparisons between PPMS patients and the other clinical forms of multiple sclerosis and healthy control subjects (Fig. 1A, B and Supplementary Table 5). Considering that *IL1B* was one of the top most expressed genes in PPMS patients and the functional enrichment observed for pathways containing *IL1B* and the *NLRP3* inflammasome among differentially expressed genes (Supplementary Table 6), we hypothesized a role for the NLRP3 inflammasome and its associated cytokine IL1B in the induction of the pro-inflammatory signature observed in patients with PPMS. In fact, a selective upregulation of *NLRP3* gene expression but not of the expression levels of genes coding for other inflammasomes such as *NLRP1*, NLR family CARD domain containing 4 (*NLRC4*), and absent in melanoma 2 (*AIM2*), was observed in PBMCs from PPMS patients compared to the other groups (Fig. 1C). RNA-seq findings were validated by real-time PCR in PBMCs from an independent replication cohort of multiple sclerosis patients and healthy control subjects. As shown in Fig. 1D, gene expression levels for *IL1B* and *NLRP3*, as well as for other cytokines identified in the pro-inflammatory signature, were again found to be significantly upregulated in PBMCs from PPMS patients compared to the other clinical forms of the disease and healthy control subjects. Based on these initial results pointing to a role for IL1B and the NLRP3 inflammasome in patients with PPMS, we carried out additional experiments to characterize the implication of the NLRP3 pathway in this particular multiple sclerosis clinical form.

Peripheral blood cell monocytes are responsible for the IL1B signature in patients with PPMS

We first investigated IL1B expression in different peripheral blood cell subsets by flow cytometry analysis. As shown in Fig. 2A, an increased frequency of IL1B-positive monocytes was found in PBMCs from PPMS patients compared to patients with ROMS and healthy control subjects, and differences were observed across the different monocyte subsets. These findings were not due to an increased relative proportion of monocytes in PPMS patients, insomuch as the frequencies of CD14 + CD16 + , CD14negCD16 + and CD14 + CD16neg monocyte subsets were similar between PPMS patients and ROMS patients (although the latter monocyte subset was significantly increased in multiple sclerosis patients compared to healthy control subjects; Supplementary Fig. 7). While low-level IL1B expression also stemmed from other PBMC subsets such as conventional or plasmacytoid dendritic cells and NK cells, only monocytes but not T or B cells displayed a unique and differential IL1B signature in PPMS patients (Fig. 2A and B). This unique IL1B monocyte-specific signature in PPMS patients was

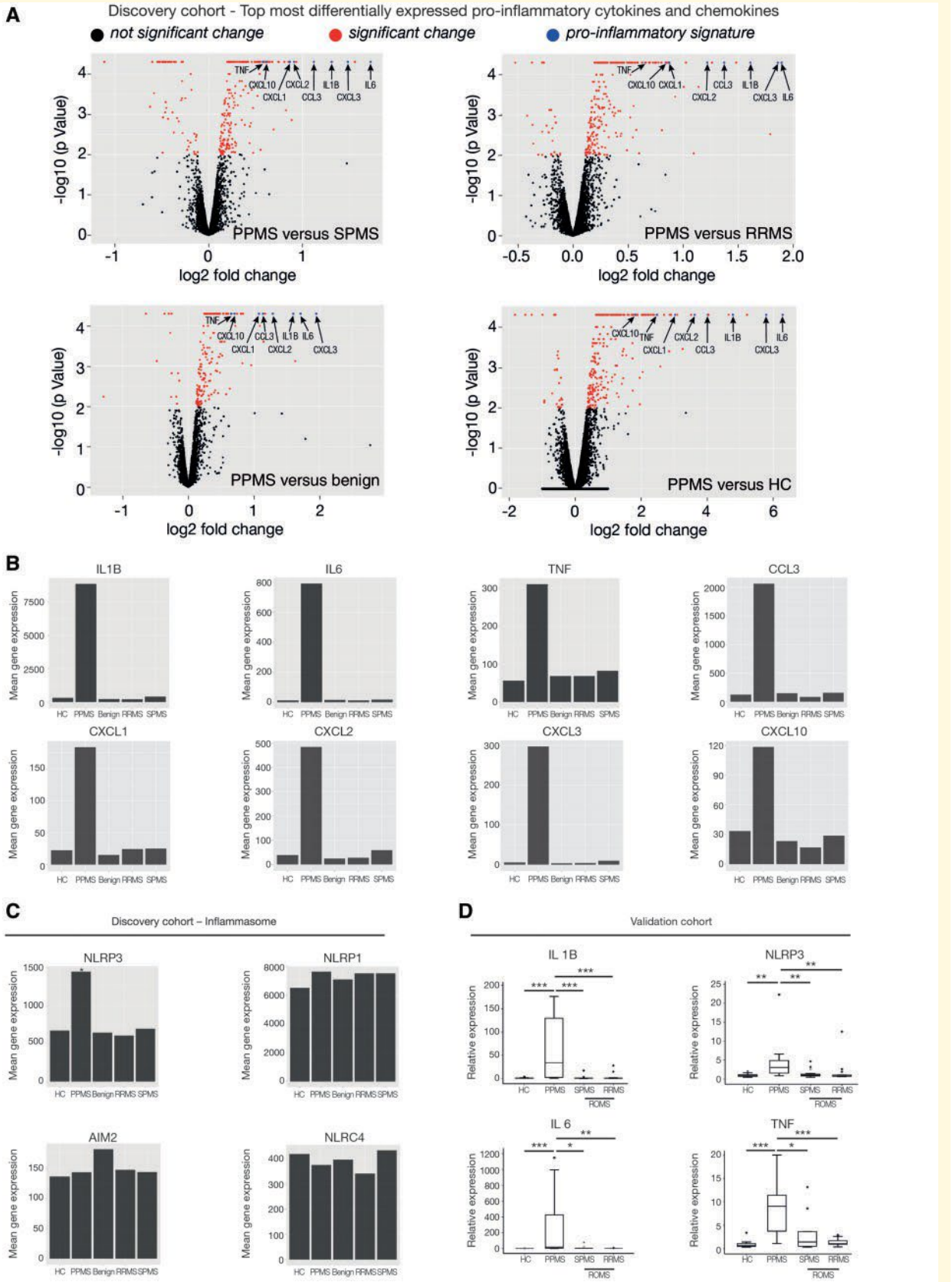

Figure 1 *IL1B* and *NLRP3* are over-expressed in PBMCs from patients with PPMS. (A–C) RNA sequencing results in a discovery cohort of 44 untreated multiple sclerosis patients [PPMS, $n = 11$; SPMS, $n = 12$; RRMS, $n = 10$; patients with benign disease course (Benign), $n = 11$] and 12 healthy controls (HC). (A) Volcano plots showing a pro-inflammatory signature formed by cytokines (*IL1B*, *TNF*, *IL6*) and chemokine genes (*CCL3*, *CXCL1*, *CXCL2*, *CXCL3*, *CXCL10*) that are consistently upregulated in all the comparisons between PPMS patients and the other clinical

(continued)

supported by the findings of similar frequencies of IL1B-related pro-inflammatory cytokines such as IL6 and TNF in monocytes from PPMS patients and other clinical forms (Fig. 2C). Further investigation on the surface expression of activation and co-stimulatory molecules such as CD80, CD86, CD40 or PD-L1 in blood cell subsets did not reveal significant differences among multiple sclerosis groups (Supplementary Fig. 8). The IL1B signature was also observed in serum, where IL1B levels were found to be elevated in PPMS patients compared to ROMS patients and healthy control subjects (Fig. 2D), and in the CSF, where the frequency of CSF IL1B positive monocytes was increased in PPMS patients compared to ROMS patients (Fig. 2E).

The NLRP3 inflammasome is more activated in PBMCs from PPMS patients

In the first instance, we investigated whether rather than activation of the NLRP3 inflammasome, differences in the IL1B signature in PPMS patients were due to increased pre-existing NLRP3 protein expression levels secondary to elevated mRNA expression levels and/or augmented signalling through the NF-jB pathway, which is known to upregulate the transcription of inflammasome components (Shao *et al.*, 2015). As shown in Fig. 3A, intracellular NLRP3 protein expression was similar between PPMS and ROMS patients across different monocyte subsets, although significantly elevated in multiple sclerosis patients compared to healthy control subjects. Likewise, an increased signalling via NF-jB was ruled out insomuch as NF-jB protein expression levels including activated NF-jB p65 were comparable between PPMS patients, ROMS patients and healthy control subjects (Fig. 3B and Supplementary Fig. 9). We next determined NLRP3 inflammasome function at baseline by measuring ASC speck formation and active caspase-1 in monocytes. As shown in Fig. 3C, caspase-1 activity was significantly increased in monocytes from both ROMS and PPMS patients compared to healthy control subjects, whereas no differences were observed between the two multiple sclerosis groups. In contrast, only PPMS patients showed significantly increased percentage of monocytes with ASC specks at baseline compared to ROMS patients and healthy control subjects (Fig. 3C). To study the canonical NLRP3 inflammasome activation in PPMS patients, PBMCs were treated with a combination of LPS and ATP, two well-known signals involved in the inflammasome pathways (Weigt *et al.*, 2017). For these experiments, a group of ROMS patients whose blood was collected at the time of clinical relapses was also included for comparison purposes (Supplementary Table 7). Similar to patients with PPMS, relapsing patients also had increased *IL1B* and *NLRP3* mRNA expression levels compared to patients in clinical remission (Fig. 3D). Following NLRP3 inflammasome stimulation, intracellular IL1B protein expression in PBMCs and IL1B levels in supernatants were highest in PPMS patients compared to ROMS patients, relapsing patients, and healthy control subjects (Fig. 3E and F). Interestingly, IL1B production from patients with PPMS was completely abrogated by incubating PBMCs with a specific NLRP3 inflammasome inhibitor (MCC950) (Coll *et al.*, 2015) (Supplementary Fig. 10A). We next investigated whether inefficient suppression of the NLRP3 inflammasome by type 1 IFN and/or IL10, which have been shown to decrease inflammasome activation and IL1B production (Guarda *et al.*, 2011; Inoue *et al.*, 2012*b*), contributed to the IL1B signature observed in PPMS patients. After a dose response study using *MX1* gene expression (MX dynamin like GTPase 1) as positive control (Supplementary Fig. 10B and C), addition of IFNb (100 IU/ml) to PBMC cultures did not result in decreased IL1B levels in supernatants of multiple sclerosis patients or healthy control subjects (Fig. 3F). In contrast, incubation of PBMCs with the anti-inflammatory cytokine IL10 significantly inhibited IL1B levels after inflammasome activation in all groups except in relapsing patients (Fig. 3F). Finally, genotyping of the rs35829419 polymorphism, whose minor allele (*A*) has been associated with an overactive NLRP3 inflammasome (Verma *et al.*, 2012), revealed similar genotype frequencies across groups (Supplementary Table 8) and ruled out a potential genetic factor due to the rs35829419 polymorphism as the cause of the higher inflammasome activation observed in PPMS patients.

High *IL1B* gene expression levels in PBMCs are associated with faster disease progression in patients with PPMS

To investigate whether *IL1B* and *NLRP3* gene expression could have prognostic implications in multiple sclerosis disease course, the time to reach a score of 6.0 in the EDSS,

Figure 1 Continued

forms of multiple sclerosis and healthy control subjects. The number of genes differentially expressed with FDR (false discovery rate)-adjusted *P*-values 5 0.05 is shown in red: PPMS versus SPMS = 396; PPMS versus RRMS = 441; PPMS versus Benign = 357; PPMS versus healthy control subjects = 569. (B) Bar graphs showing mean gene expression levels (normalized counts) of genes belonging to the pro-inflammatory signature in the different groups of multiple sclerosis patients and healthy control subjects. (C) Bar graphs with mean gene expression levels (normalized counts) of inflammasome-related genes. PPMS patients have a selective upregulation of *NLRP3* compared to the other patient categories and healthy control subjects. **P* 5 0.01. (D) Real-time PCR results in a validation cohort of 58 untreated multiple sclerosis patients (ROMS, *n* = 38; 15 SPMS and 23 RRMS) and 26 healthy control subjects. Graphs show over-expression of *IL1B*, *NLRP3*, *IL6*, and *TNF* in patients with PPMS compared to ROMS and healthy control subjects. Graphs are expressed as fold-change in gene expression in PPMS, SPMS, and RRMS relative to healthy control subjects. ****P* 5 0.001, ***P* 5 0.01, **P* 5 0.05 (Mann-Whitney U rank-sum test).

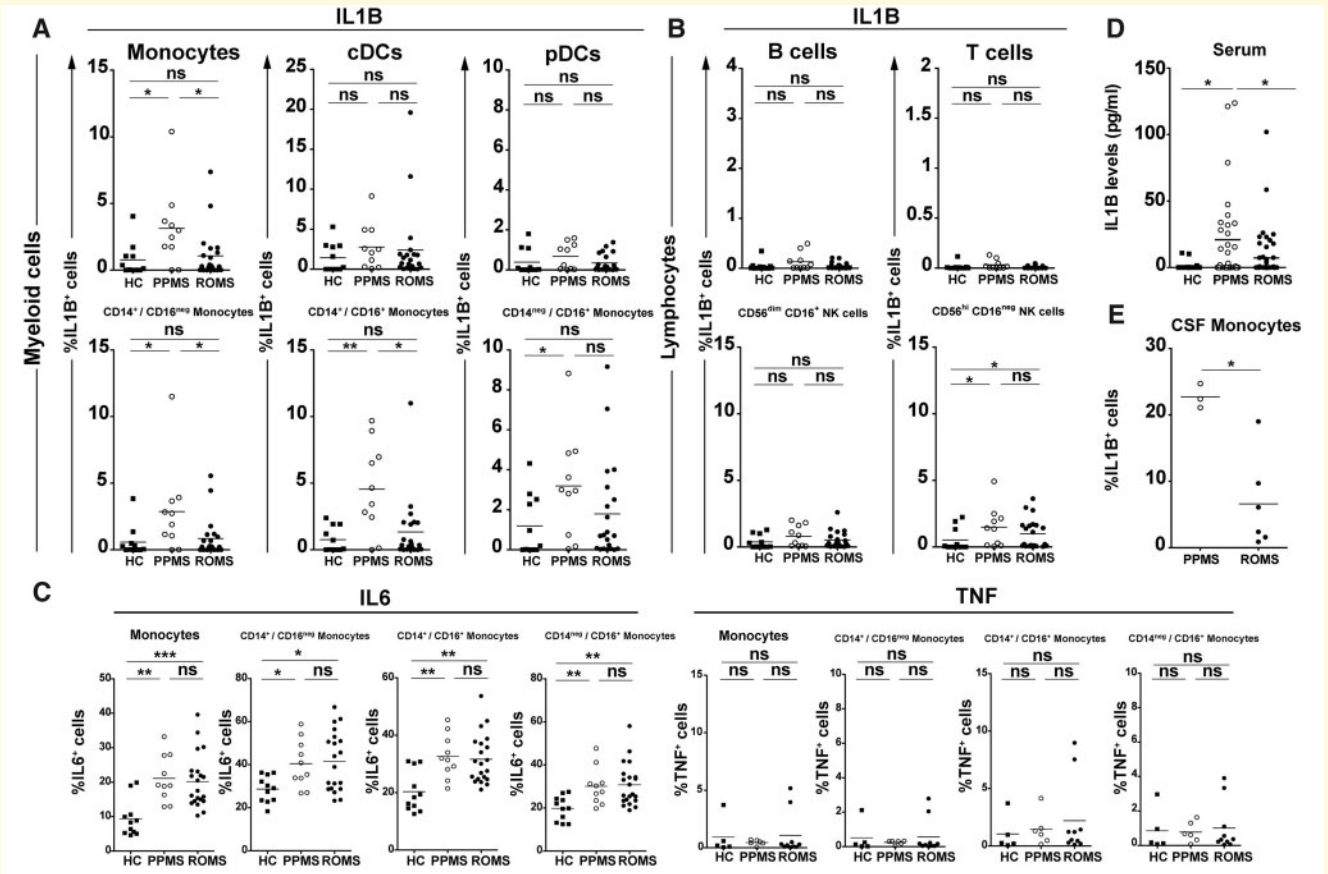

Figure 2 IL1B signature in peripheral blood monocytes, serum and CSF monocytes of patients with PPMS. (A and B) Flow cytometry analysis of intracellular cytokine expression in PBMCs reveals an increased frequency of IL1B + monocytes in PPMS patients. Graphs show the fraction of IL1B + cells within myeloid (A) and lymphoid (B) subsets from healthy controls (HC; n= 11), patients with PPMS (n= 10), and patients with ROMS (n= 21). (C) The percentage of positive monocytes expressing other cytokines such as IL6 and TNF is similar between multiple sclerosis groups. Graphs depict the fraction of IL6 + and TNF + cells in monocytes and monocyte subsets. (D) Serum IL1B levels are increased in patients with PPMS. Levels of IL1B were measured by ELISA in serum samples from healthy control subjects (n= 17), and patients with PPMS (n= 30) and ROMS (n= 51). (E) Intracellular IL1B expression determined by flow cytometry is increased in CSF monocytes from PPMS patients (n= 3) compared to ROMS patients (n= 6). In A–C, pooled data from two independent analyses are shown. Each symbol represents an individual and horizontal bars indicate mean values. ***P 5 0.001, **P 5 0.01,*P 5 0.05 by Mann-Whitney U rank-sum test. ns = P 4 0.05. cDC = conventional dendritic cells; pDC = plasmacytoid dendritic cells.

which indicates walking assistance, and the Multiple Sclerosis Severity Score (MSSS) (Roxburgh *et al.*, 2005), which relates clinical disability to disease duration, were determined in patients with high and low *IL1B* and *NLRP3* mRNA expression levels calculated according to cut-off values based on the median. As shown in Fig. 4A, PPMS patients with *IL1B* expression levels in PBMCs above the median progressed faster and reached an EDSS of 6.0 in 7 years compared to 18 years in patients having low *IL1B* levels. These findings were restricted to the PPMS group and were not observed in patients with ROMS classified according to similar criteria (Fig. 4A). In contrast, classification of multiple sclerosis patients according to *NLRP3* mRNA expression levels in PBMCs did not influence disease course of PPMS or ROMS patients (Fig. 4A). A similar prognostic picture of faster disease progression restricted both to the PPMS group and IL1B was observed using the MSSS at the time of blood collection. MSSS scores significantly correlated with *IL1B* mRNA expression levels (Supplementary Fig. 11) and were found to be higher only in PPMS patients with *IL1B* expression levels above the median compared to patients with low *IL1B* levels, but not in patients classified according to *NLRP3* expression levels (Fig. 4B and Supplementary Fig. 11). The worse disease prognosis associated with high *IL1B* mRNA expression levels in PBMCs was validated in an independent cohort of PPMS patients (Supplementary Table 3), and high *IL1B* levels were again associated with a shorter time to reach an EDSS of 6.0 compared to low *IL1B* levels (7 versus 20 years as median times, respectively) (Fig. 4C). Similarly, comparisons of MSSS scores both at the time of blood collection and at the time of last follow-up revealed significantly higher scores in PPMS patients with high *IL1B* levels compared to patients with low *IL1B* levels (Fig. 4C). Interestingly, disease progression

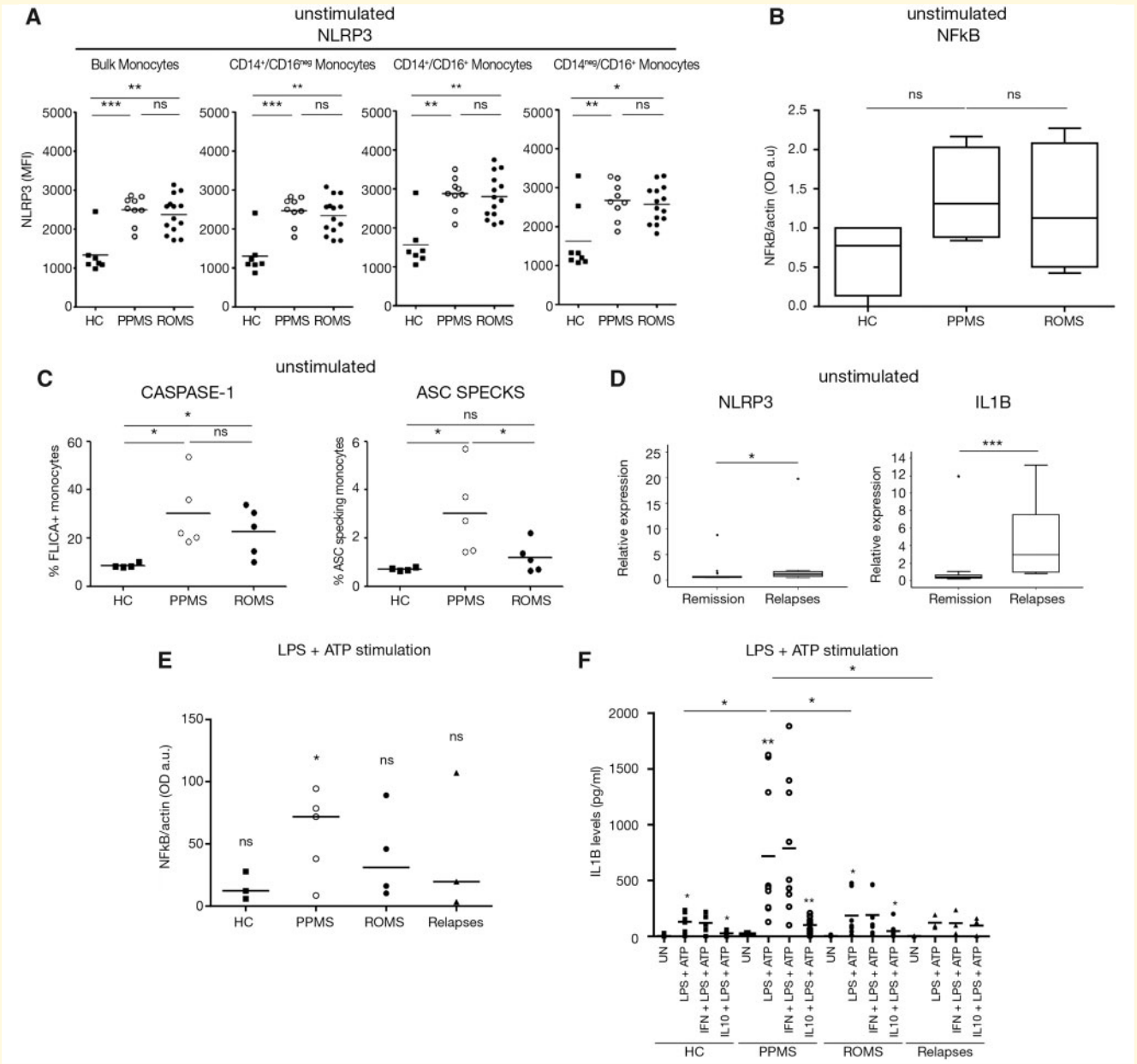

Figure 3 NLRP3 inflammasome is more activated in patients with PPMS. (A) Increased protein expression levels of NLRP3 in PBMC-derived monocytes from patients with multiple sclerosis. PBMCs from healthy controls (HC), patients with PPMS or patients with ROMS were stained for NLRP3 and its intracellular expression analysed by flow cytometry. Expression levels were compared on monocytes and monocyte subsets via median fluorescence intensity (MFI). Each symbol represents an individual. (B) NF-jB signalling pathway is not upregulated in PPMS patients. NF-jB expression levels were determined by western blot in PBMCs from PPMS patients (n= 4), ROMS (n= 4), and healthy control subjects (n= 4). Graphs represent optical densities in arbitrary units with respect to b-actin. (C) The percentage of ASC-specking CD14 + cells is increased in PPMS patients. Graphs represent the percentage of CD14 + monocytes with active caspase-1 labelled using the fluorescent inhibitor probe 660-YVAD-FMK (FLICA) staining (*left*) and the percentage of apoptosis-associated speck-like protein containing a caspase recruitment domain (ASC)-specking monocytes (*right*). Each symbol represents an individual and horizontal bars indicate mean values. (D) *NLRP3* and *IL1B* mRNA expression levels measured by real-time PCR are increased in multiple sclerosis patients during relapses compared to patients in remission. Graphs are expressed as fold-change in gene expression in ROMS patients during relapses (n= 8) relative to ROMS patients in clinical remission (n= 23). (E) IL1B expression is increased in PBMCs from PPMS patients following canonical inflammasome activation. The NLRP3 inflammasome was activated with a combination of LPS + ATP and IL1B intracellular expression was measured by western blot in PBMCs from PPMS patients (n= 5), ROMS (n= 4), relapsing patients (n= 3), and healthy control subjects (n= 3). Graphs show the median difference in IL1B expression between the unstimulated and LPS + ATP stimulated conditions represented as optical densities in arbitrary units with respect to b-actin. (F) IL1B levels are increased in supernatants of PBMCs from PPMS patients following canonical NLRP3 inflammasome activation and are inhibited by IL10 but not by IFNb. PBMCs from PPMS patients (n= 9), ROMS (n= 7), patients during relapses (n= 3), and healthy control subjects (n= 7) were stimulated with a combination of LPS + ATP alone or in the presence of IFNb (100 IU/ml) or IL10 (100 ng/ml). After inflammasome activation, supernatants were collected and IL1B levels measured by ELISA. IFN = interferon-beta; UN = unstimulated condition. Statistics: Mann-Whitney U-test. ***P 5 0.001, **P 5 0.01, *P 5 0.05, ns = P 4 0.05.

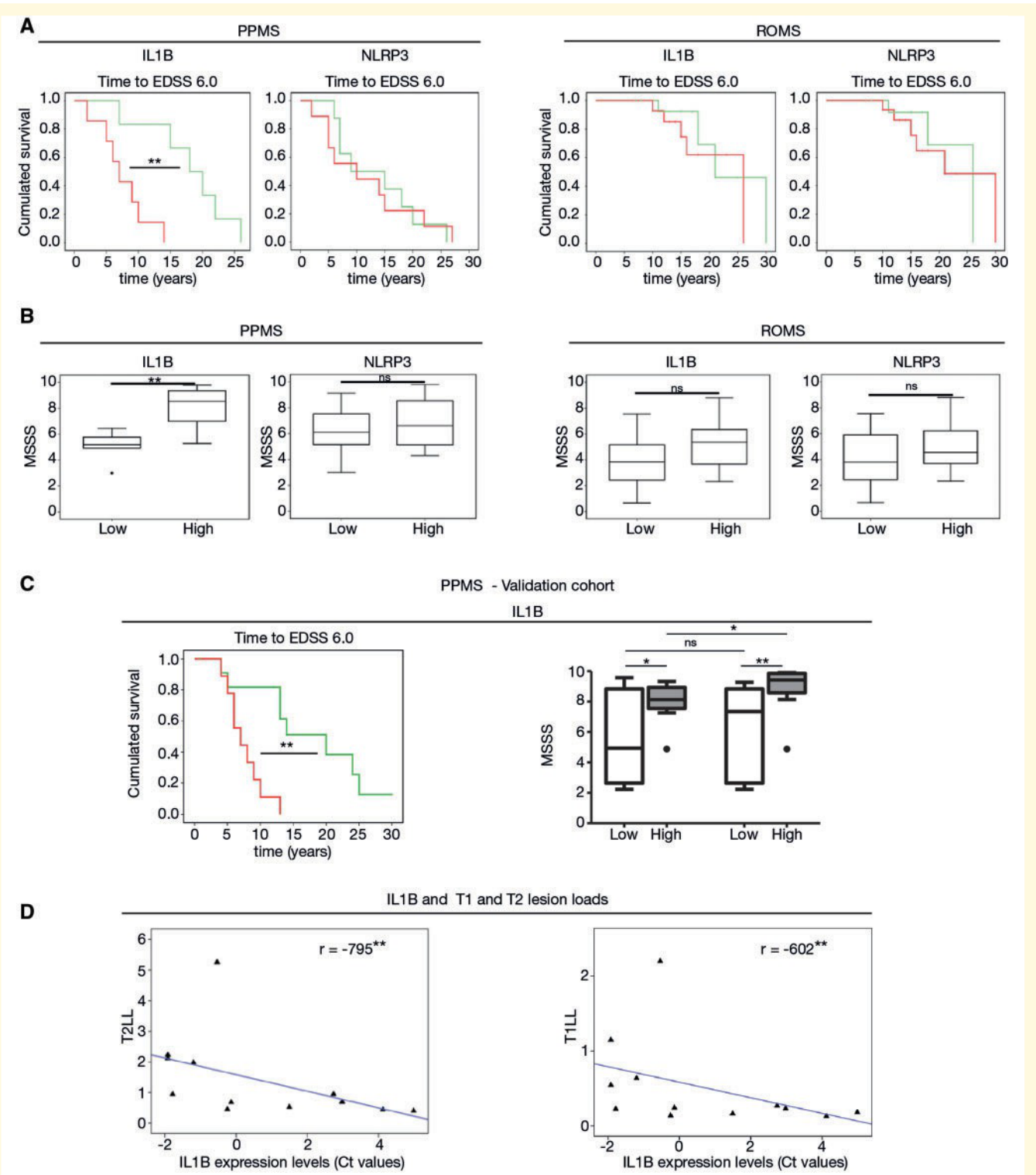

Figure 4 Patients with PPMS and high *IL1B* levels have faster disease progression. *IL1B* and *NLRP3* mRNA expression levels determined by real-time PCR in PBMCs from PPMS and ROMS patients were classified into high and low according to a cut-off value based on the median, and related to the time to reach an EDSS of 6.0 and the MSSS as outcome variables to evaluate disease progression. (A) Time to reach an EDSS of 6.0 is shorter in PPMS patients with *IL1B* levels above the median. Patients with high *IL1B* levels reached an EDSS of 6.0 [median time (95% confidence interval)] in 7.0 years (4.4–9.6) compared to 18 years (12.0–24.0) in patients with low *IL1B* levels. Statistics: log-rank test for time to EDSS 6.0. (B) MSSS scores at the time of blood collection are higher in PPMS patients with high *IL1B* levels. In PPMS patients, the median follow-up time from disease onset to blood collection was 10 years. Statistics: Mann-Whitney U-test. (C) High *IL1B* levels are associated with faster disease progression in a validation cohort of PPMS patients. Patients with high *IL1B* levels reached an EDSS of 6.0 in 7.0 years (4.1–9.9) compared to 20 years (10.3–29.7) in patients with low *IL1B* levels. *Left* boxes refer to MSSS scores at the time of blood collection 11 years as median time from disease onset. *Right* boxes refer to MSSS scores at the time of last follow-up 23 years as meadian time from disease onset.

(continued)

from the time of blood collection to the time of the last follow-up was significantly faster in PPMS patients with *IL1B* levels above the median compared to patients with low *IL1B* levels (Fig. 4C). Finally, *IL1B* mRNA expression levels in PBMCs from PPMS patients significantly correlated with brain radiological measures of lesion formation and tissue destruction such as the T_2 and T_1 lesion loads, respectively (Fig. 4D).

Both IL1B and NLRP3 are expressed in macrophages/microglial cells and associate with lesion activity in PPMS patients

We next investigated the cell source of NLRP3 and IL1B expression in brain tissue from PPMS patients. In agreement with peripheral blood findings of constrained IL1B signature in monocytes, expression of both NLRP3 and IL1B in PPMS brain tissue was mainly restricted to cells of myeloid lineage, i.e. IBA1 + macrophages/microglia. As shown in Fig. 5a, both NLRP3 and IL1B immunoreactivity was observed in IBA1 + macrophages/microglial cells located in inactive demyelinated lesions. Double immunolabelling using TMEM119 as a specific marker for microglia revealed TMEM119 downregulation on microglia associated with multiple sclerosis lesions (Supplementary Fig. 12), a finding that is in line with previous reports (Masuda *et al.*, 2019).

Interestingly, classification of PPMS brain lesions according to their demyelinating activity revealed significantly higher percentages of NLRP3 and IL1B positive cells in mixed active/inactive demyelinating lesions than in post-demyelinating lesions and brain tissue from non-neurological controls (Fig. 5B), findings that indicate an association between NLRP3 and IL1B expression and PPMS lesion activity.

NLRP3 inflammasome inhibition improves EAE and protects against axonal damage in organotypic cerebellar cultures

Based on the prognostic implications of the IL1B signature observed in PPMS patients, we next wondered whether inhibition of IL1B effects could influence EAE disease severity by using the specific NLRP3 inflammasome inhibitor MCC950 (Coll *et al.*, 2015) and the IL1 receptor (IL1R) antagonist anakinra administered in therapeutic settings (Supplementary Fig. 4 illustrates the levels of inhibition of MCC950 and anakinra). Animals were treated at Days 13–14 post-immunization, a time point in which the majority of animals had already developed clinical signs of the disease and close to the peak of *Nlrp3* and *Il1b* gene expression observed in spinal cord tissue from EAE mice (Supplementary Fig. 13). Following a dose-response study (Supplementary Fig. 14), treatment of mice with 50 mg/kg of the specific NLRP3 inflammasome inhibitor significantly attenuated EAE disease severity (Fig. 6A). This effect was not observed when mice were treated with a higher dose (100 mg/kg) of the NLRP3 inhibitor (Supplementary Table 9). Interestingly, blocking the binding of IL1B to its receptor with anakinra did not result in significant EAE improvement (Fig. 6A). Clinical improvement of mice treated with the NLRP3 inflammasome inhibitor was not associated with altered cellular immune responses, and the MOG-specific and PHA-polyclonal proliferative responses were similar between NLRP3 inhibitor-treated mice and vehicle-treated counterparts (Supplementary Fig. 15A). Likewise, IL17 production was comparable between both groups of mice (Supplementary Fig. 15B). When examining the effects of specific treatment in the CNS at the histopathological level, treatment of mice with the NLRP3 inhibitor significantly decreased the degree of inflammation and induced a modest reduction in the level of demyelination compared to the vehicle-treated group (Fig. 6B). Improvement of CNS histopathology in NLRP3-treated mice was associated with significant decrease in LEA positive macrophages/microglial cells, reduction in the number of CD3 positive lymphocytes, less astrocytosis with reduction in GFAP positive staining, and diminished axonal damage with less SMI32-positive stained area compared with vehicle-treated mice (Fig. 6C). Positive cells for NLRP3 and IL1B were mainly observed in the inflammatory infiltrates and adjacent white matter, whereas NLRP3 positive cells were also detected in the grey matter (Fig. 6C). Treatment with the specific NLRP3 inhibitor significantly reduced NLRP3 and IL1B protein expression compared to vehicle control mice (Fig. 6C). Similar to the findings in brain tissue from PPMS patients, macrophages/microglia expressed both NLRP3 and IL1B (Fig. 6D). Additionally, in EAE mice, astrocytes were also found to express both NLRP3 and IL1B and neurons showed unique expression of NLRP3 (Fig. 6D).

Considering that the PPMS form of the disease is less inflammatory compared to the relapse-onset forms (Leary and Thompson, 2005) and aiming to investigate the potential

Figure 4 Continued

Statistics: for independent samples, unpaired Student's *t*-test or Mann-Whitney U-test depending on normality of distributions; for dependent samples between MSSS assessments, Wilcoxon signed-rank test. Open and filled boxes: patients with *IL1B* levels below or above the median, respectively. (D) *IL1B* mRNA expression levels correlate with T_2-weighted lesion load (T2LL) and T_1-weighted lesion load (T1LL). r = Spearman's rank correlation coefficient. Ct (cycle threshold) value is inversely related to the amount of *IL1B* mRNA expression levels. T_2- and T_1-weighted lesion load are expressed as percentage of total brain content. Non-enhancing hypointense lesions on T_1-weighted spin echo images (black holes) were identified visually, and segmented with a semi-automated tool to obtain T1-weighted lesion load. Number of patients in A and B: PPMS, $n = 13$ for IL1B and $n = 17$ for NLRP3; ROMS, $n = 33$ for IL1B and NLRP3; 20 RRMS; and 13 SPMS. Number of patients in C and D: PPMS, $n = 21$ and $n = 12$, respectively. $^{**}P < 0.01$, $^{*}P < 0.05$, ns = $P > 0.05$.

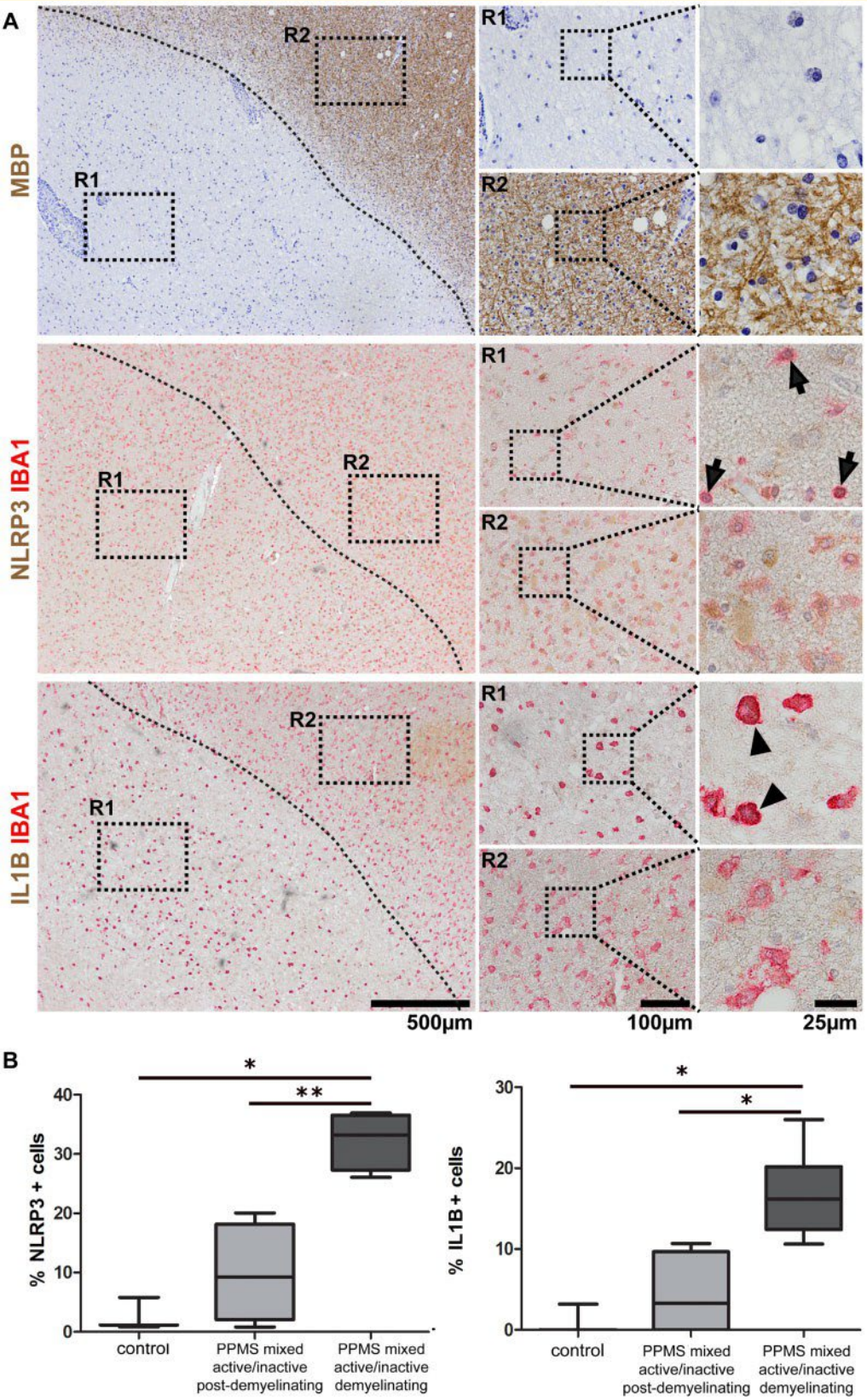

Figure 5 NLRP3 and IL1B expression in multiple sclerosis lesions. (A and B) Brain samples from PPMS patients. (A) Inactive demyelinated lesion (R1 region) classified by complete absence of MBP immunoreactivity within phagocytes according to Lucchinetti *et al.* (2000) and Masuda *et al.* (2019). NLRP3 immunoreactivity is observed in IBA1-positive cells (filled arrows) inside the lesion (R1 region) but less in the myelinated parts (R2 region). IL1B expression is detectable in IBA1-labelled macrophages/microglial cells (arrowheads) within the lesion (R1 region). Dotted lines represent the border of the demyelinated area. (B) The percentages of NLRP3 + and IL1B + cells were significantly higher in PPMS mixed active/inactive demyelinating lesions compared to PPMS mixed active/inactive post-demyelinating lesions and brain tissue from non-neurological controls. Statistics: Mann-Whitney U-test. *$P \leq 0.01$.

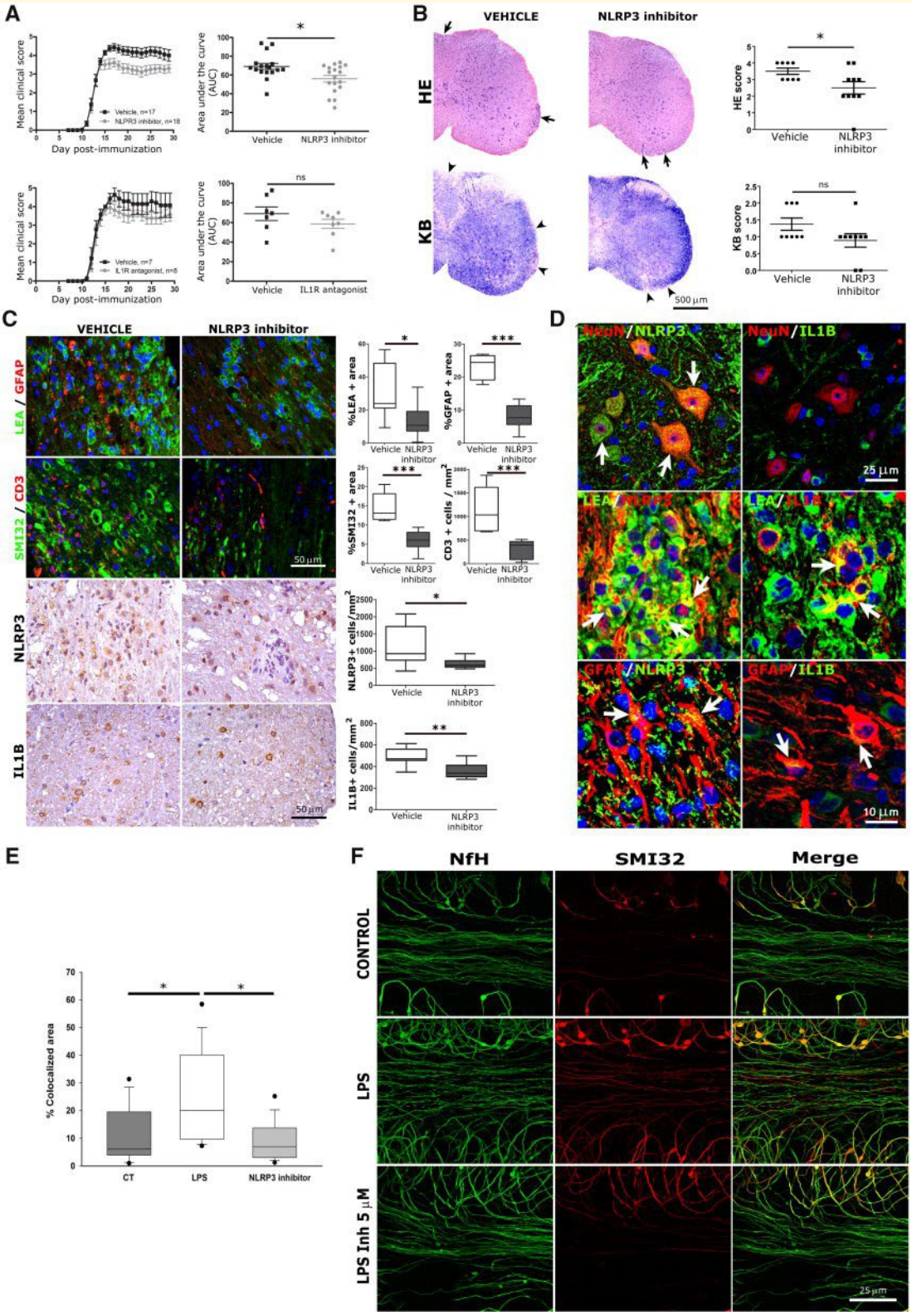

Figure 6 Treatment with the NLRP3 inflammasome inhibitor ameliorates EAE outcome and attenuates axonal damage in organotypic cultures. (A) Animals were treated at Days 13–14 post-immunization. At this point, mice were randomized into different experimental groups (vehicle, NLRP3 inhibitor or IL1R antagonist) in such a way that the clinical parameters, both the clinical and the cumulative score, were comparable at the day of randomization between all groups. Mice treated with 50 mg/kg of the NLRP3 inhibitor presented a significantly lower cumulative (57.64 ± 15.20 versus 71.24 ± 13.78, $P = 0.009$) and maximum (4.06 ± 0.57 versus 4.53 ± 0.74, $P = 0.040$) clinical score in comparison with their counterparts administered with vehicle. In contrast, treatment with the IL1R antagonist did not have a relevant impact on EAE clinical outcome. Error bars represent the standard error of the mean (SEM). Statistics: unpaired Student's *t*-test. *P 5 0.05. ns = P 4 0.05.

(continued)

role for the NLRP3 inflammasome as therapeutic target in patients with PPMS, we wondered whether specific inhibition of the NLRP3 inflammasome would still be effective in reducing axonal damage after removing the effect of the peripheral immune system in CNS pathology by using an LPS-neuroinflammation model in organotypic cerebellar cultures. Following dose-response experiments with different concentrations of the specific NLRP3 inflammasome inhibitor, a dose of 5 1M of the NLRP3-inhibitor was selected as the minimal effective dose (Supplementary Fig. 16) and found to significantly reduce the LPS-induced axonal damage evaluated by the percentage of total (phosphorylated and non-phosphorylated) heavy neurofilament (NfH) presenting non-phosphorylated NfH (SMI32) staining in cerebellar slice cultures (Fig. 6E and F).

Discussion

Inflammasomes are protein complexes that can be activated by a wide range of stimuli (Vanaja *et al.*, 2015). The NLRP3 inflammasome is the best studied of the inflammasomes and has been implicated in several autoimmune disorders including multiple sclerosis (Barclay and Shinohara, 2017). Activation of the NLRP3 inflammasome results in procaspase-1 self-cleavage to generate activated caspase-1, which then leads to maturation of IL1B and IL18 (Schroder and Tschopp, 2010). In multiple sclerosis, memory T cells from patients exhibited reduced ability to suppress NLRP3 inflammasome activation, which was restored by IFNb (Beynon *et al.*, 2012). Non-responders to IFNb were characterized by increased gene expression levels of *NLRP3* and *IL1B* in PBMCs compared to treatment responders (Malhotra *et al.*, 2015). In EAE, studies in *Nlrp3*-deficient mice have shown discrepant results, with delayed course and reduced disease severity observed in some studies (Gris *et al.*, 2010; Inoue *et al.*, 2012*a*, *b*) and protection from EAE progression in others (Shaw *et al.*, 2010; Inoue *et al.*, 2016). Whereas the discrepancies most likely adhere to differences in the immunization protocols to induce EAE, altogether these findings reflect the complexity of the NLRP3 inflammasome.

An RNA-seq approach aiming to identify multiple sclerosis disease activity biomarkers revealed a consistent IL1B signature with selective upregulation of the NLRP3 inflammasome in PBMCs from PPMS patients. While IL1B is known to be expressed by a wide range of peripheral blood cells (Zhao *et al.*, 2013), differences in IL1B expression between PPMS patients and ROMS patients and healthy control subjects were exclusively driven by monocytes. One potential explanation for the IL1B signature restricted to monocytes from PPMS patients is the presence of an overactive NLRP3-inflammasome in patients with this clinical form compared to patients with ROMS and also healthy control subjects. It should be mentioned that cytokines and chemokines included in the pro-inflammatory signature are genes induced by IL1B. The findings of increased ASC specks at baseline in monocytes from PPMS patients support this notion, as assembly of ASC into large protein oligomers is a readout for inflammasome activation (Stutz *et al.*, 2013). Interestingly, the finding of similar caspase-1 activity between PPMS and ROMS patients may suggest an NLRP3-inflammasome activation through different pathways e.g. an alternative pathway in monocytes from ROMS patients that does not require ASC speck formation but activates caspase-1 (Gaidt *et al.*, 2016). The increased IL1B levels observed after specific NLRP3-inflammasome activation with LPS and ATP is in line with a canonical NLRP3 activation in monocytes from PPMS patients. Other potential factors contributing to the IL1B signature, such as genetic factors or an insufficient response to IL10 inhibition, were excluded.

It is important to highlight that the IL1B signature associated with an overactive NLRP3 inflammasome had prognostic implications within the PPMS group but not in ROMS patients. Using the MSSS and the time to reach an EDSS of 6.0 as accepted outcome measures of disability progression (Cottrell *et al.*, 1999; Roxburgh *et al.*, 2005), PPMS patients with high *IL1B* gene expression levels in PBMCs progressed faster than those with low expression levels. Of note, a similar classification of PPMS patients according to *NLRP3* gene expression levels did not result in differences in disease progression, most likely owing to the lower dynamic range observed for NLRP3 expression levels compared with the

Figure 6 Continued

(B) Histopathology in EAE mice spinal cords. The degree of inflammation (haematoxylin and eosin, HE) (arrows) and demyelination (Klu¨ver-Barrera, KB) (arrowheads) were lower in NLRP3 inhibitor-treated animals compared with the vehicle-treated group. (C) The percentage of LEA + , GFAP + and SMI32 + area, and the number of CD3 + , NLRP3 + and IL1B + cells were significantly lower in the NLRP3 inhibitor-treated group than in the vehicle-treated group. (B and C) Statistics were done using unpaired Student's *t*-tests. ***P 5 0.001, **P 5 0.01, *P 5 0.05. ns = P 4 0.05. (D) Double immunostainings showed that both NLRP3 and IL1B were expressed in astrocytes (GFAP +) and macrophages/microglial cells (LEA +), whereas NLRP3 but not IL1B was expressed in neurons (NeuN +). Arrows indicate double positive cells. (E) The presence of 5 1M of the NLRP3 inflammasome inhibitor suppressed the axonal damage in organotypic cerebellar slices exposed to LPS (15 1g/ml) for 24 h. Boxes represent the 75th and 25th percentiles divided horizontally by the median, and error bars define the 10th and 90th percentiles. Statistics: ANOVA and Tukey's *post hoc* test. *P 5 0.01. CT = control culture condition. (F) Representative detailed images of cerebellar slices stained with phosphorylated and non-phosphorylated neurofilaments (NfH, green), non-phosphorylated neurofilaments (SMI32, red) or their superposition (merged). Scale bar = 25 1m.

dynamic range for IL1B and the tight control exerted on inflammasome activation through post-translational modifications (Groslambert and Py, 2018). Altogether these findings suggest that the determination of *IL1B* gene expression levels in PBMCs may be used as a prognostic biomarker to identify a subgroup of PPMS patients with more activated NLRP3 inflammasome and worse disease prognosis that may benefit from available multiple sclerosis therapies to delay disability progression.

In our study, immunohistochemistry assessment revealed expression of NLRP3 and IL1B in brain lesions from PPMS patients. Consistent with the IL1B signature in PBMCs, within the CNS mainly cells of the myeloid lineage, macrophages/microglia, expressed both NLRP3 and IL1B. A potential pathogenic role for NLRP3 and IL1B expression in PPMS brain lesions was supported by the correlation observed between demyelinating activity and the percentage of CNS cells positive for NLRP3 and IL1B. In line with these findings, in a cuprizone-induced demyelination mouse model, *Nlrp3* gene expression was significantly increased and mice deficient for *Nlrp3* depicted delayed demyelination and oligodendrocyte loss (Jha *et al.*, 2010). As a final point, the correlation observed in PPMS patients between *IL1B* gene expression levels and brain radiological measures of total lesion formation and tissue destruction further supports the findings in brain pathology.

Based on our findings pointing to a prognostic role of IL1B associated with NLRP3 inflammasome overactivation in patients with PPMS, we explored the potential for NLRP3 as therapeutic target in multiple sclerosis patients suffering from this progressive clinical form of the disease. We first sought to investigate the effect of inhibiting the NLRP3 inflammasome itself or blocking the IL1B binding to its receptor in EAE disease course. To block the inflammasome, we used MCC950, a selective NLRP3 inflammasome inhibitor that already proved beneficial in EAE when administered in a prophylactic setting (Coll *et al.*, 2015). To block IL1B binding, we used anakinra, a human recombinant IL-1 receptor antagonist (Dinarello, 2014). Of note, only specific inhibition of the NLRP3 inflammasome attenuated established EAE, which suggests that therapies based on specific inhibition of the NLRP3 inflammasome may result in more suitable approaches to treat progressive phases of multiple sclerosis.

Treatment with the specific inflammasome inhibitor was associated with improvement in CNS histopathology and reduction in axonal damage. The finding of similar results observed between NLRP3 inhibitor-treated and control mice for cellular immune responses and IL17 production suggest that the NLRP3 inflammasome inhibitor is attenuating EAE by reducing neuroinflammation rather than modulating peripheral immune responses. Supporting this notion, in a model of LPS-mediated axonopathy where the effect of the peripheral immune system was excluded, NLRP3 inhibition still protected against axonal damage. These findings indicate that in our model, axonal damage is mediated by IL1B and can be reduced by blocking the NLRP3 inflammasome in CNS cells. In this context, IL1B has been shown to promote neurotoxicity in EAE by increasing excitatory postsynaptic currents and inducing neuronal death in mouse corticostriatal slice cultures (Rossi *et al.*, 2012, 2014).

In summary, blood monocytes from PPMS patients are characterized by an IL1B signature secondary to canonical NLRP3 inflammasome overactivation. Segregation of PPMS patients according to their *IL1B* gene expression levels has prognostic implications insomuch as high levels are associated with faster disease progression. In brain lesions from PPMS patients, mainly cells of myeloid lineage expressed both IL1B and NLRP3 and a higher percentage of IL1B and NLRP3 positive cells correlated with lesion activity. Specific inhibition of the NLRP3 inflammasome ameliorated established EAE and protected against neuroaxonal damage. Altogether these results point to IL1B as a prognostic factor in PPMS patients and NLRP3 inflammasome as a therapeutic target, which may set the rationale for the design of specific therapies based on NLRP3 inhibition to treat patients with PPMS.

Acknowledgements

The authors would like to thank nurses, laboratory technicians and patients for their participation in samples collection. We thank Javier Mazar´ıo, Jose´ A´ ngel Rodr´ıguez-Alfaro, and Eileen Barleon for their great technical assistance.

Funding

This work was supported by a grant from the “Fondo de Investigación Sanitaria” (FIS; grant number PI16/00924), Ministry of Science and Innovation, Spain. This work was also supported by grants from the Ministry of the Economy and Competitiveness (PI15/00963; PI18/00357; MTM2015-64465-C2-1-R); Ministerio de Economı´a, Industria y Competitividad – Fondo Europeo de Desarrollo Regional (project no. SAF2017-88276-R to P.P.); European Research Council (ERC-2013-CoG 614578 to PP); Generalitat de Catalunya Suport Grups de Recerca (2017 SGR 622); Red Espan˜ola de Esclerosis Mu´ltiple (RD16/0015/0019) funded by the Fondo de Investigación Sanitaria (FIS), partially financed by F.E.D.E.R.; European Union “Una manera de hacer Europa”; and ARSEP Foundation. S.M. has been contracted from the Pla estrate`gic de recerca i innovacio´ en salut 2016–2020 (PERIS). D.C.’s group was sponsored by ADEM-TO, Aciturri Aerona´utica S.L., Vesuvius Ibe´rica and Fundacio´n Galletas Coral. D.C. and I.M. are hired by SESCAM.

Competing interests

All authors report no competing interests.

Supplementary material

Supplementary material is available at *Brain* online.

References

Baker D, Amor S. Publication guidelines for refereeing and reporting on animal use in experimental autoimmune encephalomyelitis. J Neuroimmunol 2012; 242: 78–83.

Barclay W, Shinohara ML. Inflammasome activation in multiple sclerosis and experimental autoimmune encephalomyelitis (EAE). Brain Pathol 2017; 27: 213–9.

Bermel RA, You X, Foulds P, Hyde R, Simon JH, Fisher E, et al. Predictors of long-term outcome in multiple sclerosis patients treated with interferon beta. Ann Neurol 2013; 73: 95–103.

Beynon V, Quintana FJ, Weiner HL. Activated human CD4 + CD45RO + memory T-cells indirectly inhibit NLRP3 inflammasome activation through downregulation of P2X7R signalling. PLoS One 2012; 7: e39576.

Bielekova B, Kadom N, Fisher E, Jeffries N, Ohayon J, Richert N, et al. MRI as a marker for disease heterogeneity in multiple sclerosis. Neurology 2005; 65: 1071–6.

Biomarkers Definitions Working Group. Biomarkers and surrogate endpoints: preferred definitions and conceptual framework. Clin Pharmacol Ther. 2001; 69: 89–95.

Coll RC, Robertson AA, Chae JJ, Higgins SC, Mun~oz-Planillo R, Inserra MC, et al. A small-molecule inhibitor of the NLRP3 inflammasome for the treatment of inflammatory diseases. Nat Med 2015; 21: 248–55.

Cottrell DA, Kremenchutzky M, Rice GP, Koopman WJ, Hader W, Baskerville J, et al. The natural history of multiple sclerosis: a geographically based study. 5. The clinical features and natural history of primary progressive multiple sclerosis. Brain 1999; 122: 625–39.

Comabella M, Montalban X. Body fluid biomarkers in multiple sclerosis. Lancet Neurol 2014; 13: 113–26.

di Penta A, Moreno B, Reix S, Fernandez-Diez B, Villanueva M, Errea O, et al. Oxidative stress and proinflammatory cytokines contribute to demyelination and axonal damage in a cerebellar culture model of neuroinflammation. PLoS One 2013; 8: e54722.

Dinarello CA. An expanding role for interleukin-1 blockade from gout to cancer. Mol Med 2014; 20: S43–58.

Gaidt MM, Ebert TS, Chauhan D, Schmidt T, Schmid-Burgk JL, Rapino F, et al. Human monocytes engage an alternative inflammasome pathway. Immunity 2016; 44: 833–46.

Gris D, Ye Z, Iocca HA, Wen H, Craven RR, Gris P, et al. NLRP3 plays a critical role in the development of experimental autoimmune encephalomyelitis by mediating Th1 and Th17 responses. J Immunol 2010; 185: 974–81.

Groslambert M, Py BF. Spotlight on the NLRP3 inflammasome pathway. J Inflamm Res 2018; 25: 359–74.

Guarda G, Braun M, Staehli F, Tardivel A, Mattmann C, Fo¨ rster I, et al. Type I interferon inhibits interleukin-1 production and inflammasome activation. Immunity 2011; 34: 213–23.

Inoue M, Williams KL, Gunn MD, Shinohara ML. NLRP3 inflammasome induces chemotactic immune cell migration to the CNS in experimental autoimmune encephalomyelitis. Proc Natl Acad Sci USA 2012a; 109: 10480–5.

Inoue M, Williams KL, Oliver T, Vandenabeele P, Rajan JV, Miao EA, et al. Interferon-b therapy against EAE is effective only when development of the disease depends on the NLRP3 inflammasome. Sci Signal 2012b; 5: ra38.

Inoue M, Chen PH, Siecinski S, Li QJ, Liu C, Steinman L, et al. An interferon-b-resistant and NLRP3 inflammasome-independent subtype of EAE with neuronal damage. Nat Neurosci 2016; 19: 1599–609.

Jha S, Srivastava SY, Brickey WJ, Iocca H, Toews A, Morrison JP, et al. The inflammasome sensor, NLRP3, regulates CNS inflammation and demyelination via caspase-1 and interleukin-18. J Neurosci 2010; 30: 15811–20.

Kuhlmann T, Ludwin S, Prat A, Antel J, Bru¨ ck W, Lassmann H. An updated histological classification system for multiple sclerosis lesions. Acta Neuropathol 2017; 133: 13–24.

Leary SM, Thompson AJ. Primary progressive multiple sclerosis: current and future treatment options. CNS Drugs 2005; 19: 369–76.

Livak KJ, Schmittgen TD. Analysis of relative gene expression data using real-time quantitative PCR and the 2(-Delta Delta C(T)) Method. Methods 2001; 25: 402–8.

Lublin FD, Reingold SC. Defining the clinical course of multiple sclerosis: results of an international survey. Neurology 1996; 46: 907–11.

Lucchinetti C, Bru¨ ck W, Parisi J, Scheithauer B, Rodriguez M, Lassmann H. Heterogeneity of multiple sclerosis lesions: implications for the pathogenesis of demyelination. Ann Neurol 2000; 47: 707–17.

Malhotra S, R´ıo J, Urcelay E, Nurtdinov R, Bustamante MF, Ferna´ndez O, et al. NLRP3 inflammasome is associated with the response to IFN-b in patients with multiple sclerosis. Brain 2015; 138: 644–52.

Masuda T, Sankowski R, Staszewski O, Bo¨ ttcher C, Amann LS, et al. Spatial and temporal heterogeneity of mouse and human microglia at single-cell resolution. Nature 2019; 556: 388–92.

Montalban X, Sastre-Garriga J, Tintore´ M, Brieva L, Aymerich FX, Rı´o J, et al. A single-center, randomized, double-blind, placebo-controlled study of interferon beta-1b on primary progressive and transitional multiple sclerosis. Mult Scler 2009; 15: 1195–20.

Rossi S, Furlan R, De Chiara V, Motta C, Studer V, Mori F, et al. Interleukin-1b causes synaptic hyperexcitability in multiple sclerosis. Ann Neurol 2012; 71: 76–83.

Rossi S, Motta C, Studer V, Macchiarulo G, Volpe E, Barbieri F, et al. Interleukin-1b causes exitotoxic neurodegeneration and multiple sclerosis disease progression by activating the apoptotic protein p53. Mol Neurodegener 2014; 9: 56.

Roxburgh RH, Seaman SR, Masterman T, Hensiek AE, Sawcer SJ, Vukusic S, et al. Multiple Sclerosis Severity Score: using disability and disease duration to rate disease severity. Neurology 2005; 64: 1144–51.

Schroder K, Tschopp J. The inflammasomes. Cell 2010; 140: 821–32.

Shao BZ, Xu ZQ, Han BZ, Su DF, Liu C. NLRP3 inflammasome and its inhibitors: a review. Front Pharmacol 2015; 6: 262.

Shaw PJ, Lukens JR, Burns S, Chi H, McGargill MA, Kanneganti TD, et al. Cutting edge: critical role for PYCARD/ASC in the development of experimental autoimmune encephalomyelitis. J Immunol 2010; 184: 4610–4.

Stutz A, Horvath GL, Monks BG, Latz E. ASC speck formation as a readout for inflammasome activation. Methods Mol Biol 2013; 1050: 91–101.

Trapnell C, Pachter L, Salzberg SL. TopHat: discovering splice junctions with RNA-Seq. Bioinformatics 2009; 25: 1105–11.

Vanaja SK, Rathinam VA, Fitzgerald KA. Mechanisms of inflammasome activation: recent advances and novel insights. Trends Cell Biol 2015; 25: 308–15.

Verma D, Sa¨ rndahl E, Andersson H, Eriksson P, Fredrikson M, Jo¨ nsson JI, et al. The Q705K polymorphism in NLRP3 is a gain-of-function alteration leading to excessive interleukin-1b and IL-18 production. PLoS One 2012; 7: e34977.

Weigt SS, Palchevskiy V, Belperio JA. Inflammasomes and IL-1 biology in the pathogenesis of allograft dysfunction. J Clin Invest 2017; 127: 2022–9.

Zhao R, Zhou H, Su SB. A critical role for interleukin-1b in the progression of autoimmune diseases. Int Immunopharmacol 2013; 17: 658–69.